Supporting Information –
Estimating the Thermodynamic Contribution to Recent Greenland Ice Sheet Surface Mass Loss

Jonathon R. Preece[1], Patrick Alexander[2,3], Thomas L. Mote [1], Gabriel J. Kooperman[1], Xavier Fettweis [4], and Marco Tedesco [2,3,]

[1]Department of Geography, University of Georgia, Athens, 30602, USA.
[2] Lamont-Doherty Earth Observatory, Columbia University, Palisades, 10964, USA.
[3] NASA Goddard Institute for Space Studies, New York, 10025, USA.
[4]Laboratory of Climatology, Department of Geography, SPHERES research unit, University of Liège, Liège, Belgium

Correspondence to: Jonathon R. Preece (jonathon.preece@uga.edu)

Abstract. The Greenland Ice Sheet has become the largest single frozen source of global sea level rise following a pronounced increase in meltwater runoff in recent decades. The pivotal role of anomalous anticyclonic circulation patterns in facilitating this increase has been widely documented; however, this change in atmospheric circulation has coincided with a rapidly warming Arctic. While amplified warming at high latitudes has undoubtedly contributed to trends in Greenland's mass loss, the contribution of this shift in background conditions relative to changes in regional circulation patterns has yet to be quantified. Here, we apply the pseudo-global warming method of dynamical downscaling to estimate the contribution of the change in the thermodynamic background state under global warming to observed Greenland Ice Sheet surface mass loss since the turn of the century. Our analysis demonstrates that, had the recent atmospheric dynamical forcing of the Greenland Ice Sheet occurred under a preindustrial setting, anomalous surface mass loss would have been reduced by over 62% relative to observations. We show that the change in the thermodynamic environment under amplified Arctic warming has augmented melt of the ice sheet via longwave radiative effects accompanying an increase in atmospheric water vapor content. Furthermore, the thermodynamic contribution to surface mass loss over the exceptional melt years of 2012 and 2019 was less than half that of the long-term average, demonstrating a reduced influence during periods of strong synoptic-scale atmospheric forcing.

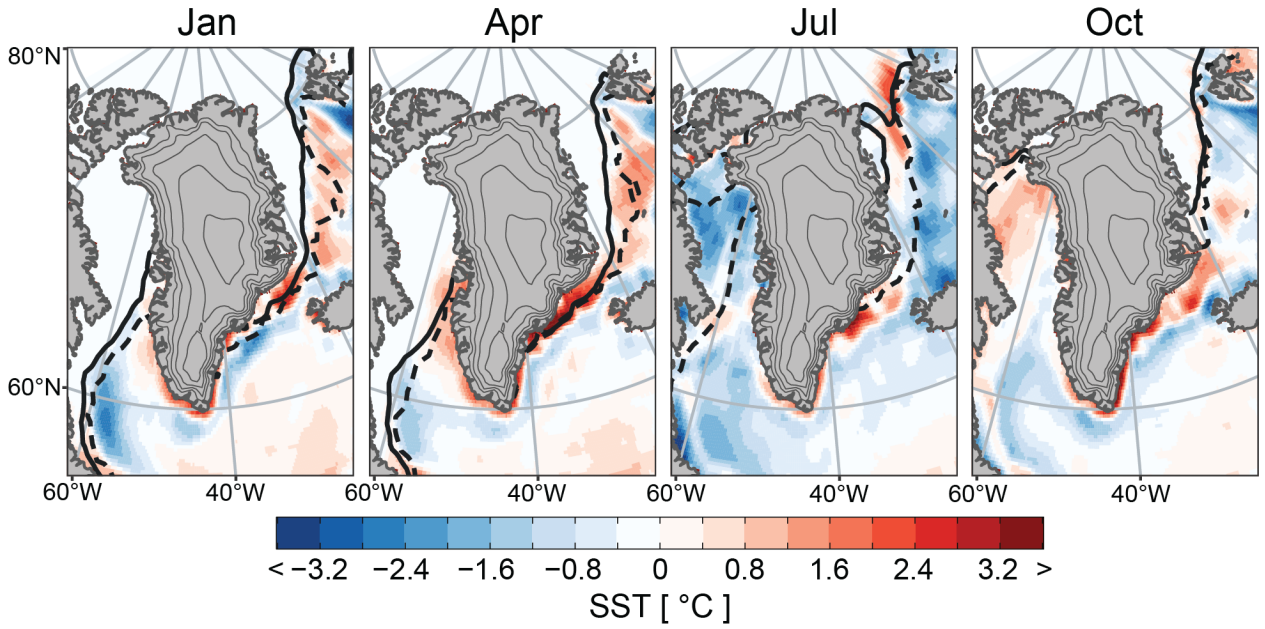

Figure S1: Change in sea-surface conditions around Greenland. Maps show the difference in SST (shading) and the location of the sea ice edge (black contours) between the prescribed 1880-1899 Hadley-OI fields used in the PGW experiments and the 2000-2019 ERA5 sea-surface conditions used in the control. Differences are shown for a selection of months equally spaced throughout the year as labeled at the top of each panel. Positive values (red shading) indicate warmer SST during the preindustrial period than during the control. White shading indicates either no change or areas of 100% SIC. Solid contour demarcates the sea ice edge for the control period, dashed for the preindustrial period. Sea ice edge is defined using a threshold of ≥ 50% SIC.

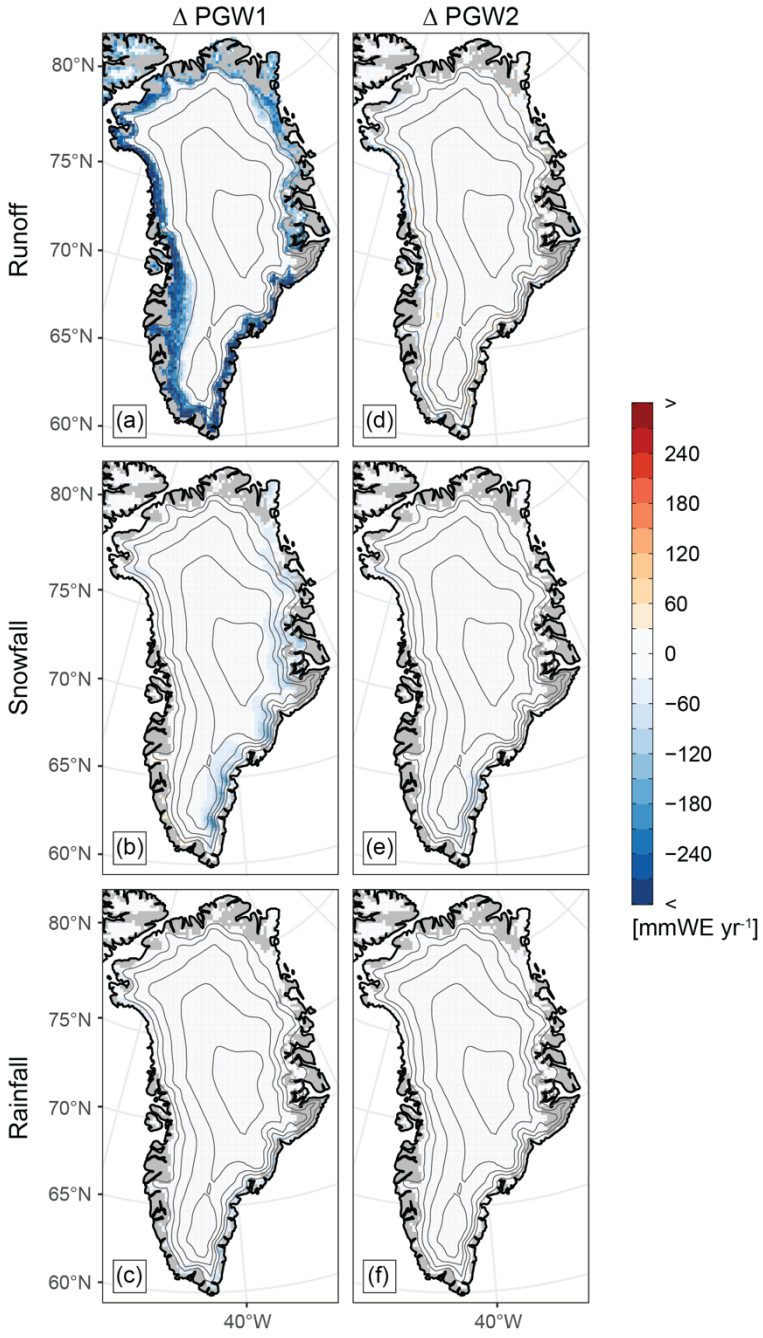

Figure S2: Comparison of individual SMB terms between the PGW simulations and the control. (a–c) difference between PGW1 and the control, (d–f) difference between PGW2 and the control for each SEB component as organized by row as labeled to the left: (a, d) runoff; (b, e) snowfall; (c, f) rainfall. Δ = PGW − Control. Contour interval: 500 m. Range: 1000–3000 m.

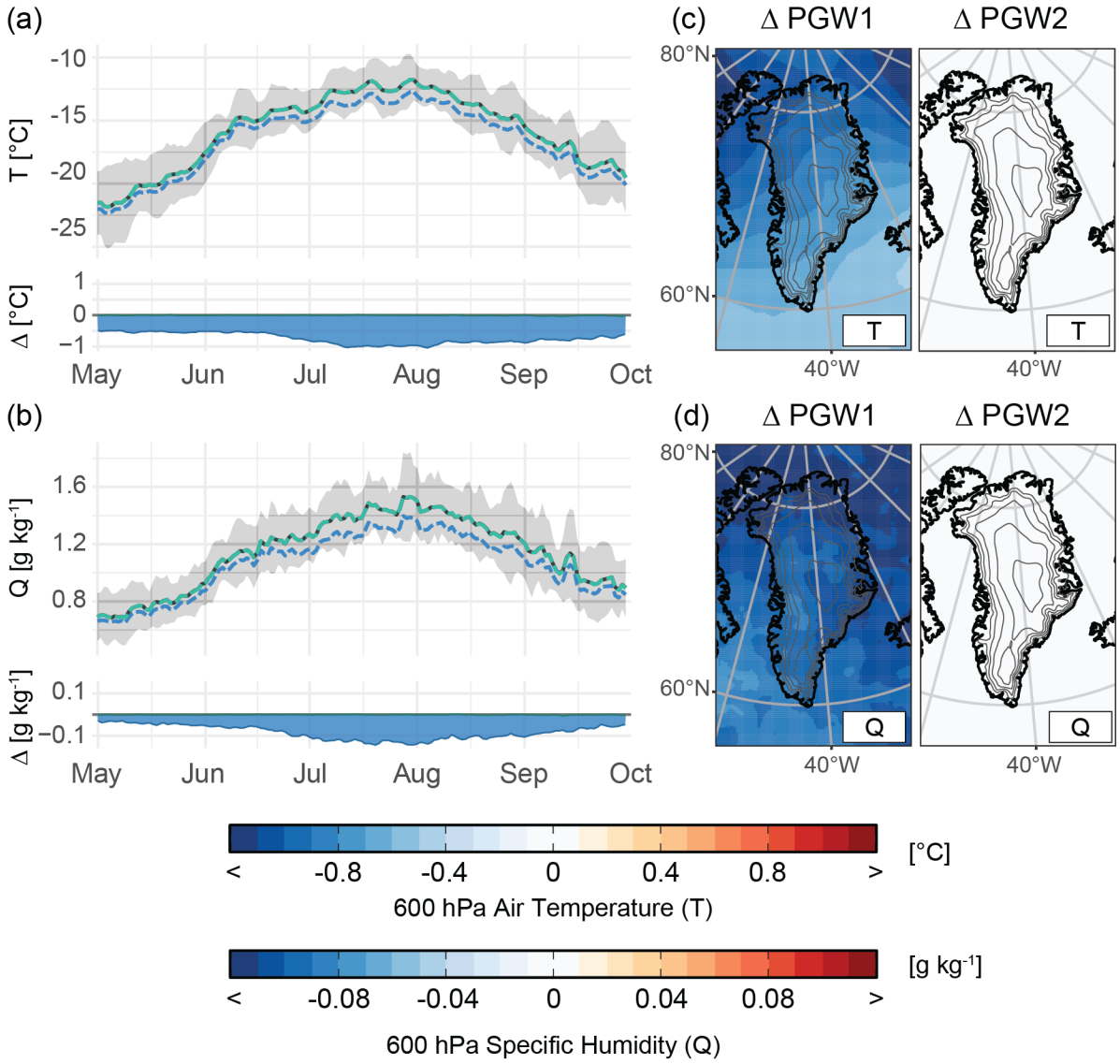

Figure S3: As in Fig. 7 but for 600 hPa (a, c) air temperature (T) and (b, d) specific humidity (Q).

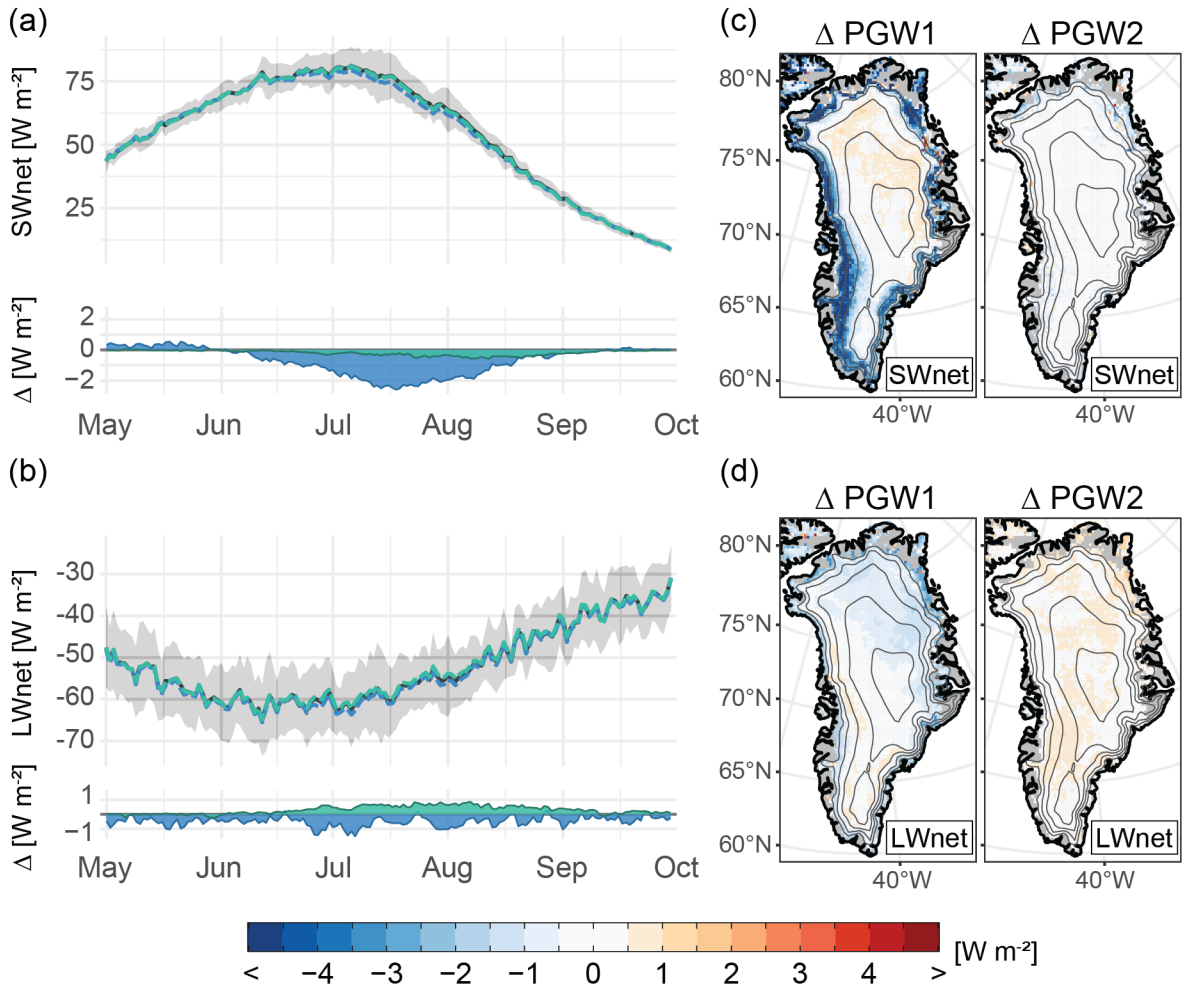

45 **Figure S4:** As in Fig. 7 but for the net radiative components: (a, c) net shortwave radiation (SWnet). (b, d) net longwave radiation (LWnet). In each case, net values are computed as downwelling minus upwelling radiation.